Dose distribution in cardiac catheterization laboratory (CathLab). Monte Carlo calculations vs TLD measurements

Kamil Kisielewicz[1,ABCDEGH], *Adrian Truszkiewicz*[2,BCD], *Sebastian Wach*[BCD], *Anna Dziecichowicz*[1,BCD], *Maciej Budzanowski*[3,CF]

[1] National Institute of Oncology Krakow Branch, Garncarska 11, 31-115 Krakow, Poland
[2] Clinical Regional Hospital No 2 in Rzeszow, Lwowska 60, 35-301 Rzeszow, Poland
[3] Institute of Nuclear Physics, Polish Academy of Sciences, Radzikowskiego 152, Krakow, Poland

Abstract

Purpose. Cardiac catheterization and angiography interventional procedures lead to higher exposures of patients and personnel than do other procedures in diagnostic radiology. The aim of these MC simulation and measurements was to obtain a 3-D dose distribution at some distance around the X-ray unit, generated during standard interventional cardiology procedures.

Matherials and Methods. In an effort to evaluate X-ray doses received by the medical staff in a catheterization unit of a cardiology department, Monte Carlo calculation using MCNPX code was performed. Exposures were also measured in air using thermoluminescent dosimeters (TLD) within a three-dimensional grid of about 100 regularly spaced measurement points placed inside the operating room. Curtains containing about 100 dosimeters forming a grid were placed as close to the X-ray equipment as possible for a period of time involving several routine catheterizations (using phantom of patient). This part of the project was intended to highlight areas of the highest X-ray exposure during catheterization, of relevance to the positioning of the medical personnel around the operating table during this procedure. In all measurements, standard TL badges used for environmental monitoring, calibrated in units of air kerma in water, each containing three high-sensitive MCP-N (LiF:Mg,Cu,P) detectors, were used.

Results. Results of environmental measurements were compared with dose distributions calculated using the MCNPX (Monte Carlo N–Particle X Transport) Code. The MCNPX simulation included coherent and incoherent scattering as well as photoelectric absorption effects. Comparison between TLD measurements and MCNPX calculations was made at selected measurement points. Comparison of MC calculation and TL measurements shows differences between the compared values: -42% to +33% with mean weighted value of 15%.

Conclusions. MC calculation, even for a simplified model, can be used to determinate areas important for radiation protection in cathlab operating room.

Key words: hemodynamics, angiography, radiation distribution, radiation protection, TLD measurements, Monte Carlo calculation, MCNPX, scattered radiation, interventional radiology, invasive cardiology.

Introduction

According to EC Directive 2013/59 [1], Polish Atomic Law[2] and implementing regulations[3], Health Care Centres using X-ray equipment in diagnostics and interventional radiology are obligated to optimize radiological exposures and to perform employee and patient dosimetry and necessary quality control tests. For every interventional X-Ray equipment, dose distribution around the device must be known for typical working conditions. Interventional cardiology is the most common interventional radiology procedure in all European countries[(4)]. The main goal of this work is to compare Monte Carlo (MC) calculated

Medicine Physicist & Engineer 1/2026 vol. 1

received: 12.05.2026; corrected: 20.05.2026; accepted: 25.05.2026

Author Contributions:
A – Conceptualization, B – Validation, C – Formal analysis, D – Resources, E – Writing—original draft preparation, F – Writing—review and editing, G – Visualization, H – Supervision.
All authors have read and agreed to the published version of the manuscript.

dose distribution and actual environmental dosimetry (using thermo-luminescence dosimeters - TLD) during interventional cardiology procedures. Such calculation and measurements are especially important for the Cathetery Lab's employees[15]. Determining the most dangerous areas in the lab will help minimizing radiation influence on employees' bodies. Results of the comparison of MC Calculation (even for a simplified model) and TL measurements show that Monte Carlo approach may be used to estimate dose distribution in an operating room (lab).

Materials and methods

Monte Carlo Calculation

Monte Carlo codes base on probability theory. MC codes predict energy deposition, most probable tracks of particles and photons going through the matter as well as interactions between them. It is a very useful tool for medical physics problems: radiotherapy planning, radiation shields designing, radioisotope production and others. There are many MC codes. The most popular are PENELOPE (developed in Barcelona), GEANT4 (CERN, EGSNRC) and MCNP. MCNPX is a Monte Carlo general-purpose transport code based on MCNP. MCNPX project was started in 1994 in Los Alamos National Laboratory (USA) as a MCNP4B and LATEH extension. MCNPX offers better, enhanced physical models for all particles and photons, new cross section data for physical interactions[17]. MCNPX support coherent and incoherent scattering as well as photoelectric absorption effects. It offers also new variantion reduction methods[16], which decrease computation time.

MCNPX in our project was used to calculate scattered dose distribution around X-Ray unit in an interventional (invasive) cardiology operating room, during a typical cardio-angiography procedure. To perform MC calculation, geometrical model of operating room as well as X-Ray beam spectrum is essential. All the information is described in an input file, according to MCNPX rules. Geometrical CathLab is modelled using boxes, right circular cylinders and planes. Using Boolean operators, patient table, C-arm, X-Ray tube, image receptor, patient phantom and operating room have been defined. For each element of CathLab, geometry (patient couch, C-arm, water phantom, etc.), atomic compositions and material densities were defined. For example:

Patient phantom is a cube filled with water. Our material has a density of 1g/ccm. Water is modelled as 2 atoms of hydrogen and 1 atom of oxygen. Atomic number of hydrogen is 1, oxygen is 8. The part of code defining materials and geometry is presented below:

c m4 - water d=1.000 g/ccm - definition of water, having density d.

m4 1000 2 8000 1 - atomic composition of material - m4 (water): 2 atoms of hydrogen (1000), 1 atom of oxygen (800).

box -95 -20 102 100 0 0 0 40 0 0 0 20 - patient phantom: first three numbers are the corner coordinates, the next numbers are the vectors coordinates. Three vectors fixed in one corner have to be defined.

This way, 3D CathLab environment has been created.

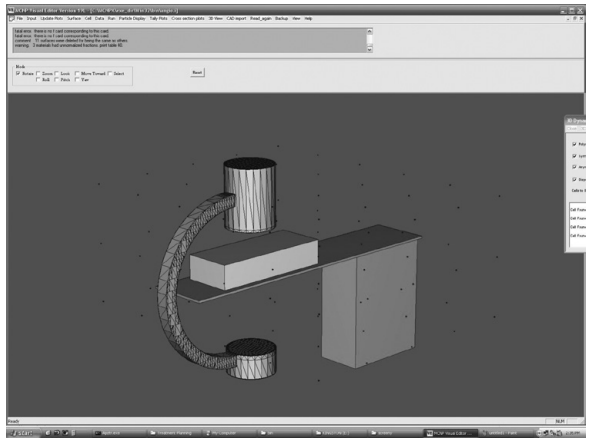

Fig. 1 *Geometrical model of CathLab (VisEd - MCNP Visual Editor) Source. Own.*

Material of X-Ray tube, C-arm, image receptor, and patient couch was defined as a polyamide (to simplify the model). Thermoluminescence dosimeters were defined as spheres filled with air due to TL material energy transfer coefficient. Such an approach is simple and sufficient for the presented model of operating room.

The source of X-Ray radiation was a diagnostic X-Ray tube with the peak energy of 80 keV. Minimum spectrum energy took into account was 8 keV. Theta angle for selected tube was 30 degree. Air thickness to the water surface was 100 cm, beryllium window thickness of the tube used was 0.8 mm. As an additional filtration, 2.5 mm of aluminum and 0.11 mm of copper were used. X-Ray beam energy spectrum was generated using SpekCalc software (by Gavin G. Poludniowski - Institute of Cancer Research and The Royal Marsden NHS Foundation Trust) for the defined anode material and tube filtration. Output spectrum file presents energy [keV] versus photon counts [photon cnts. / keV ccm mAs].

Energy spectrum is defined and presented as a histogram. Using energy bin equal to 1 keV allows to observe only K alpha and K beta characteristics lines. It is a good solution for precalculation for its short computation time. For a final calculation, 0.2 keV energy bin was used. This is more precise, but also more time consuming. This time, we observed much sharper characteristic lines. Moreover, K alpha 1and 2, and K beta 1 and 2 spectra lines were observed.

The next step was to separate characteristic radiation lines from braking radiation to make the calculations *stand-alone.*

Calculations were performed for 10E9 iterations each.

As a result, MC calculation returns value of probability density function [MeV/g] in a quoted point-specific tallie..

After normalization (maximum value is equalled to 1 for graphics presentation and comparison with TLD readouts), dose distribution map has been created. In fact, distribution

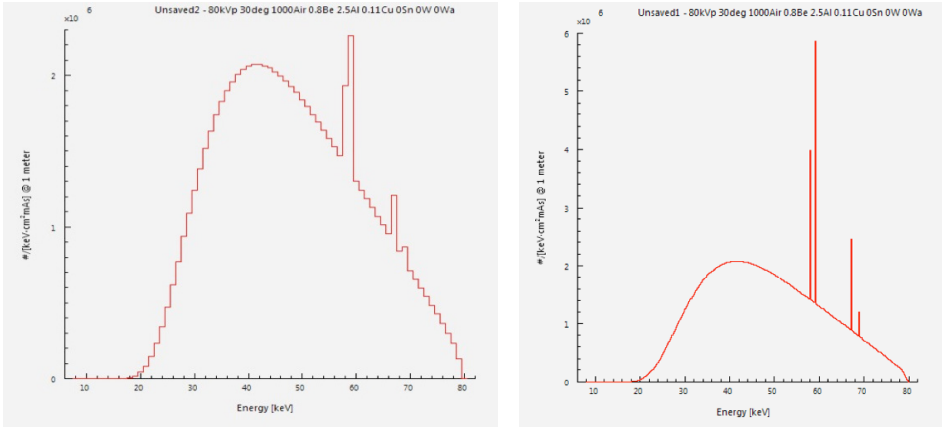

Fig. 2 *Used energy bin: a) 1 keV for precalculation, b) 0.2 keV for final calculation*
Source. Own.

of probability density function is presented. It corresponds to the dose. Computations were performed for typical coronary artery imaging C-arm projections (described below after measurements section).

Measurements

Three dimensional radiation distribution was measured using environmental passive dosimeters with high sensitive thermoluminescent detectors based on MCP-N (LiF:Mg,Cu,P) . Every TL badge (measurement point being a single dosimeter) contains 3 TL detectors. The measurement experiment was performed using four curtians of TL dosmeters. On three of the curtains, dosemeters were placed at four height levels: 0.6 m, 1.1 m, 1.6 m, and 2.1 m above the floor. The first curtain had only three levels of 0.6 m, 1.1 m and 1.6 m. The first courtain contained 21 dosemeters, while the second and the third 28 badges each. On the last curtain, there were 22 measurement points. Positions of MC tallies were geometrically defined in the same positions as TL badges during measurements. The result is the comparison of normalized values for specific MC tallies and respective TL measurement points.

Dose distribution was measured only within the cube of 3.5x2x2 m^3 around the X-ray tube and patient couch so as to get more information about radiological risk near the tube and operating table. To avoid disturbing the staff during the actual medical procedure, a water phantom was used to simulate the patient's body. For every curtain, a set of seven C-arm projections usually used in coronaro-artery imaging were performed:

- LAO (Left Anterior Oblique) 90°,
- LAO 60°,
- LAO 35°, CAUDAL 30°,
- LAO 0° , CRANIAL 30°,
- LAO 0°, CAUDAL 30°,
- RAO (Right Anterior Oblique) 30°, CAUDAL 0° - two times performed,
- LAO 40°, CRANIAL 20°.

Each projection was acquired in contrast recording mode (with high value of current (mA)). Projection time for each C-arm position was 10 seconds. After completing eight-exposure sequence, curtains were moved 0.5m forward and dosimeters were replaced. Geometry implemented in Monte Carlo calculation included the described C-arm positions. Dose in a single measurement point is measured as a total dose after all the exposures.

Using Mathlab software, linear interpolation has been performed every 0.1 m for measurements points and calculated MC tallies. Interpolated results have been visualised using Gnuplot software.

Results

Based on the results from TL detectors curtains, horizontal and vertical scans (along and across the patient couch) have been reconstructed. After 80 seconds of radiation (8 cine exposures, 10-second long each), the maximum dose acquired by detectors on the curtains was near to the water phantom. On the dose distribution map (Fig. 3,4), a regular scatter radiation around the phantom is observed. At the 1.1m level, additional scatter radiation from shielding element is recorded.

Results from MC calculation are very similar and correspond well with TL measurements. Calculated dose gradient is much wider compared to the measurements.

Monte Carlo computation uncertainties have been estimated as a standard deviation (SD) of mean tallie value.

TLD measurements uncertainties u(K_a) have been estimated as a cumulative uncertainty described below.

$$u(K_a) = \sqrt{\left(0{,}025 \cdot \frac{\overline{I_{POM\_NET}}}{\overline{I_{NET}}}\right)^2 + \left(u\left(\overline{I_{NET}}\right) \cdot \left(-\frac{K_{aKAL} \cdot \overline{I_{POM\_NET}}}{\overline{I_{NET}}^2}\right)\right)^2 + \left(u\left(\overline{I_{POM\_NET}}\right) \cdot \frac{K_{aKAL}}{\overline{I_{NET}}}\right)^2}$$

Where:

K_{aKAL} – known value of air kerma during calibration, calibration dose

I_{NET} – counts corresponding to calibration dose,

I_{POM_NET} – average value of counts for unknown dose (unknown air kerma)

$u(I_{POM\_NET})$ – standard uncertainty for I_{POM_NET},

$u(I_{NET})$ – standard uncertainty for I_{NET},

Calculated uncertainties for MC computation range from 20% up to 50%. TLD measurements uncertainties were estimated as 5% of the measured air kerma (for the used dose range, up to 0.1 mGy).

Uncertainties for specific TLD-MC point pairs are presented in Table 1.

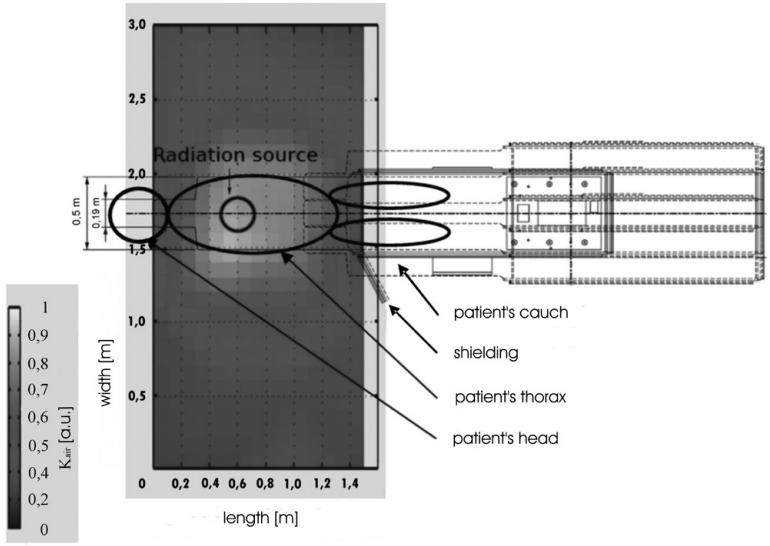

Fig. 3 *Horizontal dose distribution map at couch level – TLD measurements*
Source: Own.

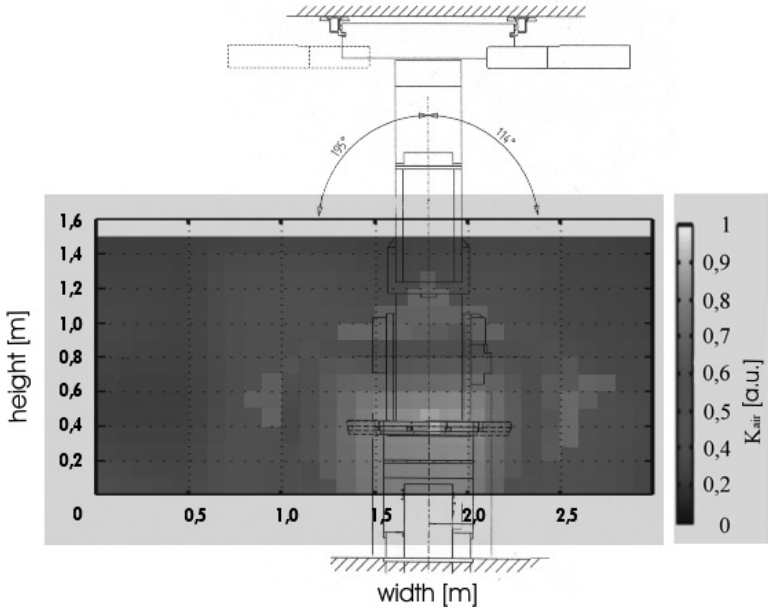

Fig. 4 *Vertical dose distribution map, layer along patient couch - MCNPX calculation*
Source: Own.

Table 1 *MCNPX calculation vs. TLD measurements*

tallie	Cell	MCNPX [MeV/g]	Uncertainty MCNPX (Std. dev.) [%]	TLD [mGy]	Cumulative uncertainty of TLD [mGy]	Cumulative uncertainty of TLD [%]	MCNPX after normalization [a.u.]	TLD after normalization [a.u.]	MCNPX vs. TLD [%]
f106:p	10	3.20E-08	47	0.07	0.02	29	0.15	0.21	31
f116:p	11	4.23E-08	38	0.09	0.03	33	0.19	0.27	29
f126:p	12	1.78E-07	26	0.30	0.06	20	0.81	0.91	11
f136:p	13	1.78E-07	36	0.30	0.09	30	0.81	0.91	11
f146:p	14	5.70E-08	41	0.10	0.03	30	0.26	0.30	14
f156:p	15	3.01E-08	44	0.06	0.03	50	0.14	0.18	25
f166:p	16	2.37E-08	32	0.05	0.02	40	0.11	0.15	29
f176:p	17	4.63E-08	38	0.10	0.03	30	0.21	0.30	30
f186:p	18	2.20E-07	29	0.33	0.03	9	1.00	1.00	0
f196:p	19	1.86E-07	33	0.31	0.09	29	0.85	0.94	10
f206:p	20	6.35E-08	44	0.13	0.02	15	0.29	0.39	27
f216:p	21	2.90E-08	48	0.06	0.04	67	0.13	0.18	27
f226:p	22	3.23E-08	26	0.07	0.03	43	0.15	0.21	31
f236:p	23	4.48E-08	32	0.10	0.03	30	0.20	0.30	33
f246:p	24	1.78E-07	28	0.30	0.05	17	0.81	0.91	11
f256:p	25	1.77E-07	41	0.29	0.05	17	0.81	0.88	8
f266:p	26	4.56E-08	37	0.08	0.08	100	0.21	0.24	14
f276:p	27	2.79E-08	22	0.06	0.04	67	0.13	0.18	30
f286:p	28	1.24E-08	30	0.07	0.02	29	0.27	0.23	-17
f296:p	29	1.32E-08	26	0.09	0.02	22	0.29	0.30	3
f306:p	30	4.36E-08	36	0.30	0.04	13	0.96	1.00	4
f316:p	31	4.36E-08	21	0.30	0.05	17	0.96	1.00	4
f326:p	32	2.12E-08	40	0.12	0.05	42	0.47	0.40	-17
f336:p	33	1.06E-08	29	0.06	0.03	50	0.23	0.20	-17
f346:p	34	9.43E-09	33	0.07	0.03	43	0.21	0.23	11
f356:p	35	4.44E-08	19	0.30	0.06	20	0.98	1.00	2
f366:p	36	2.50E-08	17	0.17	0.02	12	0.55	0.57	3
f376:p	37	1.53E-08	21	0.11	0.06	55	0.34	0.37	8
f386:p	38	1.18E-08	32	0.09	0.03	33	0.26	0.30	13
f396:p	39	9.61E-09	28	0.07	0.02	29	0.21	0.23	9
f406:p	40	1.28E-08	34	0.07	0.02	29	0.28	0.23	-21
f416:p	41	2.72E-08	34	0.17	0.02	12	0.60	0.57	-6
f426:p	42	4.48E-08	41	0.25	0.03	12	0.99	0.83	-18
f436:p	43	4.54E-08	22	0.28	0.08	29	1.00	0.93	-7
f446:p	44	1.30E-08	19	0.06	0.03	50	0.29	0.20	-43
f456:p	45	1.29E-08	36	0.06	0.03	50	0.28	0.20	-42
f946:p	94	1.62E-08	34	0.08	0.04	50	0.26	0.22	-18
f956:p	95	2.73E-08	30	0.15	0.02	13	0.44	0.42	-6
f966:p	96	6.11E-08	44	0.36	0.03	8	0.99	1.00	1
f976:p	97	6.17E-08	41	0.33	0.03	9	1.00	0.92	-9
f986:p	98	2.92E-08	37	0.15	0.02	13	0.47	0.42	-14
f996:p	99	1.48E-08	36	0.09	0.04	44	0.24	0.25	4
f1006:p	100	1.32E-08	31	0.07	0.02	29	0.21	0.19	-10
f1016:p	101	1.96E-08	40	0.13	0.04	31	0.32	0.36	12
f1026:p	102	2.60E-08	24	0.15	0.02	13	0.42	0.42	-1
f1036:p	103	2.63E-08	28	0.17	0.02	12	0.43	0.47	10
f1046:p	104	2.21E-08	23	0.14	0.02	14	0.36	0.39	8
f1056:p	105	1.38E-08	36	0.07	0.03	43	0.22	0.19	-15
f1066:p	106	1.44E-08	28	0.08	0.03	38	0.23	0.22	-5
f1076:p	107	2.17E-08	39	0.12	0.05	42	0.35	0.33	-6
f1086:p	108	2.36E-08	44	0.13	0.05	38	0.38	0.36	-6
f1096:p	109	3.07E-08	41	0.15	0.02	13	0.50	0.42	-19
f1106:p	110	2.17E-08	23	0.12	0.04	33	0.35	0.33	-6
f1116:p	111	1.70E-08	38	0.09	0.03	33	0.28	0.25	-10

Source: Own.

Conclusion

As shown in Table 1, the lower detection limit for the used TL dosimeters is approx. 0.06 mGy. MCNPX gives more stepped differentiation down to the lowest values (Fig. 4).

The results obtained from TL detectors readout show that the dose distribution of X-Ray radiation at 0.6 m, 1.1 m, and 1.6 m hight levels correspond to patient (phantom) and couch location (along the patient couch). The influence of different X-Ray projections on the dose shape is not so significant due to scattered radiation (from phantom, patient couch and shields). Measured Air Kerma generally comes from scattered radiation.

The comparison of MCNPX calculation and TL measurements shows differences between the compared values: -42% to +33% with mean weighted value of 15%. MC calculation even for a simplified model can be used to determine areas of importance to radiation protection as an alternative to environmental radiation measurements. We observed that patient's body is a source of scattered radiation. Radiation shields proved to be properly designed because they protect physician's working area from scattered photons. In case of activities carried out near patient's head (injections), personnel is not protected as lead shield are mounted below patient's thorax. Therefore, proper training and experience of CathLab stuff is essential for minimizing radiation risk during hemodynamic procedures. In many departments, additional lead shields need to be designed and installed for specific medical procedures to protect stuff sufficiently. Some of the procedures also need optimizing, e.g. when contrast recording mode is used, there is high dose rate so personnel should move 3 steps backward or leave the operating room. Consciousness of radiation risk can optimize workflow in CathLab and reduce doses absorbed by both patients, and stuff[18].

References

1. COUNCIL DIRECTIVE 2013/59/EURATOM
2. Polish Atomic Law (in Polish: Dz. U. 2026, poz. 1).
3. Regulation of the Polish Minister of Health on the conditions for safe application of ionizing radiation in medical exposures (in Polish: Dz. U. 2023 poz. 195).
4. Schmidt T, Wucherer M, Results of an European Action on Risk Evaluation in Interventional Radiology and a First · Attempt for Reference Value – Course, Radiation Protection in Interventional Radiology. Madrit; May 1997. p. 121131.
5. International Commission of Radiation Protection. 1990 Recommendations of the International Commission on Radiological Protection. ICRP Publication 60. Pergamon Press; 1991.
6. International Commission of Radiation Protection. General principles of monitoring for radiation protection of workers. ICRP Publication 75. Pergamon Press; 1997.
7. Padovani R, Rodella CA. Staff dosimetry in interventional cardiology. Radiat Prot Dosimetry. 2001;94(12):99103.
8. International Commission on Radiation Units and Measurements. Quantities and units in radiation protection dosimetry. ICRU Report 51. Oxford University Press; 1993.
9. Faulkner K. Radiation protection in interventional radiology. Br J Radiol. 1997;70:325326.
10. Martin CJ. A review of radiology staff doses and dose monitoring requirements. Radiat Prot Dosimetry. 2009;136(3):140157.
11. Hendricks JS et al. MCNP Extensions Version 2.5.0. MCNPX Handbook. Los Alamos National Laboratory; April 2005.
12. Pelowitz DB. MCNPX User Manual Version 2.5.0. Los Alamos National Laboratory; April 2005.
13. Poludniowski G et al. SpekCalc: a program to calculate photon spectra from tungsten anode xray tubes. Phys Med Biol. 2009;54.
14. Carinou E et al. Monte Carlo calculations on extremity and eye lens dosimetry for medical staff at interventional radiology procedures. Radiat Prot Dosimetry. 2011;144(14):492496.
15. Siiskonen T et al. Occupational radiation doses in interventional radiology: simulations. Radiat Prot Dosimetry. 2008;129(13):3638.
16. Ferrari P et al. Evaluation of the dose to the patient and medical staff in interventional cardiology employing computational models. Radiat Prot Dosimetry. 2010;141(1):8285.
17. Gallmeier FX. An improved photoabsorption cross section model for the physics models regime in MCNPX. Radiat Prot Dosimetry. 2005;116(14):264269.
18. Budzanowski M et al. Dose levels of the occupational radiation exposures in Poland based on results from the accredited dosimetry service at the IFJ PAN, Kraków. Radiat Prot Dosimetry. 2011;144(14):107110.